Publication P6

Sami Ruoho, Timo Santa-Nokki, Jere Kolehmainen, and Antero Arkkio. 2009. Modeling magnet length in 2-D finite-element analysis of electric machines. IEEE Transactions on Magnetics, volume 45, number 8, pages 3114-3120.

© 2009 Institute of Electrical and Electronics Engineers (IEEE)

Reprinted, with permission, from IEEE.

This material is posted here with permission of the IEEE. Such permission of the IEEE does not in any way imply IEEE endorsement of any of Aalto University's products or services. Internal or personal use of this material is permitted. However, permission to reprint/republish this material for advertising or promotional purposes or for creating new collective works for resale or redistribution must be obtained from the IEEE by writing to pubs-permissions@ieee.org.

By choosing to view this document, you agree to all provisions of the copyright laws protecting it.

Modeling Magnet Length In 2-D Finite-Element Analysis of Electric Machines

Sami Ruoho[1,2], Timo Santa-Nokki[3], Jere Kolehmainen[4], and Antero Arkkio[1]

[1]Department of Electrical Engineering, Helsinki University of Technology, FIN-02015 TKK, Finland
[2]Neorem Magnets Oy, FIN-28400 Ulvila, Finland
[3]Magnet Technology Centre, Prizztech Oy, Pori, Finland
[4]ABB Oy, Motors, Vaasa, Finland

Two-dimensional finite-element-method (2-D FEM) calculations are widely used in electric machine modeling instead of three-dimensional calculations because of their faster calculation time and simplicity. However, the 2-D calculations ignore end effects, causing a large error in calculating eddy currents in permanent magnets of synchronous machines. In this paper, we develop three analytical models and one curve-fitting model based on numerical calculations. The models improve the eddy-current loss calculation accuracy in 2-D FEM. The method adjusts the resistivity of a magnet material according to magnet dimensions. The adjustment takes into account the resistivity, the temperature dependence, and anisotropy of the resistivity of rare-earth magnet materials. We compare the models against FEM calculations in two and three dimensions and show that all the models improve the eddy-current loss calculation accuracy significantly, especially when the time-harmonic caused eddy-current losses in permanent magnets are considered.

Index Terms—**Eddy current, finite-element analysis, magnetic field modeling, permanent magnets.**

I. Introduction

An eddy-current calculation of an electric machine is a three-dimensional (3-D) problem by its nature. However, 3-D analytic calculations are possible in a few geometries only, and 3-D finite-element-method (FEM) calculations can still be far too time consuming in a practical design work. For this reason, two-dimensional (2-D) analytic and finite-element eddy-current calculations are widely used.

A radial-flux electric machine has a transversal symmetry along the axis of rotation, which makes 2-D calculations reasonable: the calculated geometry is the middle cut-plane of the machine. For longer machines this 2-D approximation gives better results, because the end effects of the machine do not have such an influence on the total performance. For eddy-current calculations of the permanent-magnet machine, however, the situation is different: for practical manufacturing reasons, the largest dimension of modern permanent magnets normally is around 100 mm, while a modern large machine in MW category can have a rotor around 1 m long [1]. It is also possible that magnets in a machine are axially cut to pieces to reduce eddy currents [2], [3]. In each magnet, there exists an axial eddy current in the magnet sides but also a circumferential eddy current at the magnet ends, which is excluded from 2-D calculations. These circumferential eddy currents in adjacent magnet ends almost cancel each other from the field solution point of view, but these currents still cause losses (Fig. 1). Because of this, the 2-D finite-element analysis of permanent-magnet machine does not give accurate results, when eddy currents in permanent magnets are considered.

The 2-D finite-element analysis still is far more computationally efficient than the 3-D finite-element analysis. Analytical equations are naturally even more effective in use. Thus, it makes sense to use 2-D analysis or analytical equations in eddy-current calculations of electric machines. Markovic and Perriard have compared analytical and 2-D FEM eddy-current calculations in a slotless cylindrical machine configuration [4], [5].

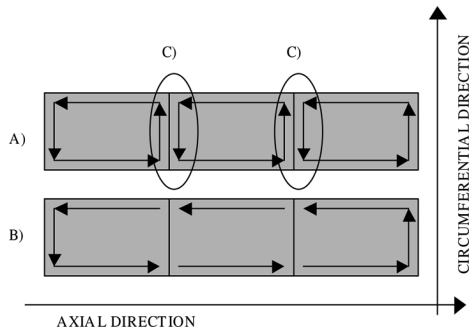

Fig. 1. Eddy currents in an axial row of magnets in a radial-flux machine (a). Circumferential eddy currents in permanent magnets almost cancel each other in the middle magnet ends (b) making 2-D approximation solid from the field solution point of view. These circumferential currents still cause losses (c) making 2-D approximation inaccurate from the eddy-current point of view.

The goal of this study is to develop an analytical model, which improves the eddy-current loss calculation accuracy in 2-D finite-element analysis when compared to similar 3-D analysis. The method used is to adjust the electric resistivity of permanent-magnet material according to the magnet dimensions. This idea of adjusting resistivity has been used before by Kesavamurthy *et al.* [6] in calculating a solid rotor induction motors and by Deak *et al.* [7], [8] for permanent-magnet motors. In the present study, the resistivity will be adjusted also according to the magnet temperature and the anisotropy of resistivity of Nd–Fe–B material [9].

II. Sources of Eddy-Current Losses

Eddy currents in permanent magnets in an electric machine are mainly caused by two reasons: time-harmonics by nonsinusoidal input waveform and space-harmonics by nonconstant re-

Manuscript received September 30, 2008; revised February 19, 2009. Current version published July 22, 2009. Corresponding author: S. Ruoho (e-mail: sami.ruoho@tkk.fi).

Digital Object Identifier 10.1109/TMAG.2009.2018621

0018-9464/$26.00 © 2009 IEEE

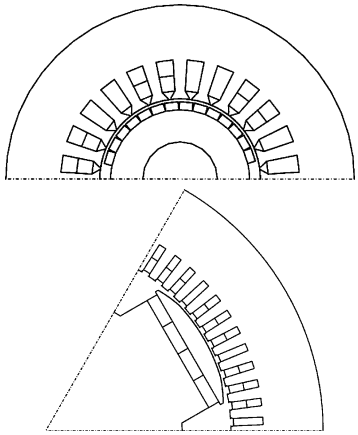

Fig. 2. Machine geometries used to estimate the relative importance of time-harmonics and space-harmonics. The topmost machine is a two-pole machine of 60 kW. The machine on the bottom is a six-pole salient-pole machine of 720 kW.

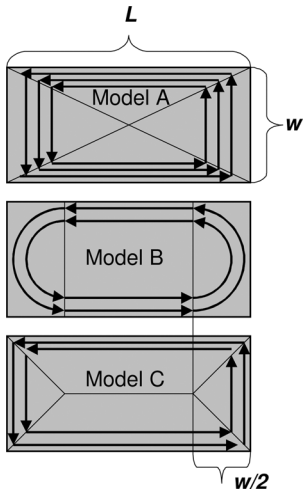

Fig. 3. Eddy-current path in a magnet in models A, B, and C.

luctance because of stator slotting [7], [10]. In this paper, the terms "time-harmonics" and "space-harmonics" are based on the stator point of view.

In this section, the relative importance of different eddy-current sources is studied by calculating the eddy-current losses in permanent magnets with two different machine geometries (Fig. 2) using 2-D FEM:

- 60 kW, 9000 rpm, 400 V, two-pole machine with 14 magnets circumferentially in one pole;
- 720 kW, 240 rpm, 690 V, six-pole salient-pole design with pole shoes.

The machines were first fed with the sinusoidal input waveform and then with the pulsewidth modulation (PWM) waveform. The eddy-current losses in the magnets were calculated in both the cases. By comparing the results, the relative importance of the different eddy-current sources for the machines can be studied.

The eddy-current losses in the permanent magnets with sinusoidal input are caused by the space-harmonics only, because the synchronous sinusoidal input does not cause any time-varying field in the rotor. The eddy-current losses with PWM input are caused with both the space-harmonics and time-harmonics. The harmonic frequencies of the input current are causing a time-varying field in the rotor, causing long-wave time-harmonics. However, the harmonics of the input current also increase the significance of the space-harmonics in the rotor. Thus, it is not possible to completely separate the source of the eddy-current losses.

The eddy-current losses in the magnets of the two-pole machine were 37 W with the sinusoidal input waveform and 480 W with the PWM input. The results for the six-pole design were 1 W and 620 W, respectively. Thus, it can be seen, that the eddy current caused by the space-harmonics with the sinusoidal input current are a lot smaller than the eddy-current losses with the PWM input, including both time-harmonics and space-harmonics.

III. Analytical Models

In this section, three analytical models are derived to calculate the eddy-current loss caused by time-harmonics in permanent magnets in 3-D. A magnet in a rotor is normally wider than one stator slot pitch in a traditionally wound machine, thus the eddy currents caused by stator slotting form several loops in a single magnet, while eddy currents caused by time-harmonics form a single eddy-current loop in a magnet. The assumptions made when deriving these equations limit the study to eddy currents caused by time-harmonics. The 2-D- and 3-D-models derived here are based on the following assumptions.

- The magnetic flux density B is uniform throughout a magnet.
- The problem is resistance limited, i.e., the frequency is relatively low.
- The eddy current flows in one plane, i.e., the eddy-current density is the same through the thickness h.

A. 2-D Model

Polinder and Hoeijimakers have derived a formula for eddy-current loss density [11], [12] (A1 in the Appendix). The eddy-current loss in a magnet with dimensions L, w, and h (length, width, and thickness, respectively) is presented in (A2) of the Appendix.

B. 3-D Models

Three equations to calculate the eddy-current loss in 3-D cases are derived. Model A assumes that the eddy current flows parallel to the magnet sides, and then turns 90° at the diagonal line of the magnet (Fig. 3). Model B assumes that the eddy current flows parallel to the magnet sides in the middle of a magnet, but at the ends of the magnet, the eddy current flows a circular path (Fig. 3). The third model, model C, assumes that the eddy current flows parallel to the magnet sides in the middle of a magnet, but at the ends of the magnet, the eddy current turns 90° at a line coming from a magnet corned at an angle of 45° respective to the magnet end (Fig. 3). All three—(A3), (A4), and (A5)—are presented in the Appendix.

IV. Numerical Calculations

A. Simulations

To compare the results of the 3-D and 2-D eddy-current calculations, a generic numerical model for 3-D and 2-D FEM

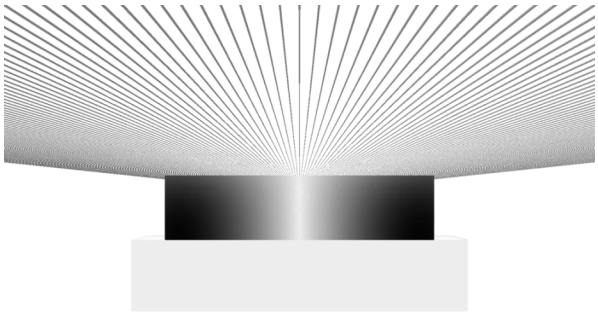

Fig. 4. Structure of a model used to define correction factor between 2-D and 3-D eddy-current losses numerically. There is a magnet on the top of an iron plate. Above the magnet there is an array of conductors.

calculations was designed (Fig. 4). The model represents one pole length of a surface magnet machine. In the model, there is a block of permanent-magnet material on nonconductive soft iron. The magnet was modeled as a nonmagnetized, but conductive object. Above the magnet, there is a row of conductors, which were fed with sinusoidal currents. The phase difference between different conductors was such that the flux density created a standing half-wave on the magnet. The magnet width was 80% of this half-wavelength, which is a typical magnet width relative to the pole width.

Both 3-D and 2-D modeling were done by using a commercial 3-D FEM software. The 2-D modeling was obtained from the 3-D model just by changing the boundary conditions at the magnet ends. In the 2-D model the current density was set to be perpendicular to the magnet end along the length, while in the 3-D model the current density was set to be parallel to the magnet length.

Three different magnet sizes were modeled (length $\times$ width $\times$ height):

- $75 \times 75 \times 18$ mm^3
- $50 \times 18 \times 8$ mm^3
- $50 \times 62 \times 8$ mm^3.

B. Results

The simulations were performed by changing one variable at a time. The changed variables were the mechanical dimensions of the magnet and the input frequency. In every case, the eddy-current loss in a magnet was calculated both in three and two dimensions.

At low frequencies, the 2-D calculations gave too-high eddy-current losses compared to the 3-D results, but at higher frequencies, the situation changes: The losses given by 3-D calculations were higher than the losses given by 2-D calculations in higher frequencies. The loss ratio between 3-D and 2-D calculations can be found in Fig. 5 for all the three modeled magnet sizes.

When the applied frequency is small, the eddy-current loss ratio between the 3-D- and 2-D-calculations remains approximately constant, as can be seen in Fig. 5. In these cases, the problem is clearly resistance limited.

A number of simulations were done by changing only the magnet length but keeping the width and height constant and the input frequency at 100 Hz. It was noted that the loss ratio

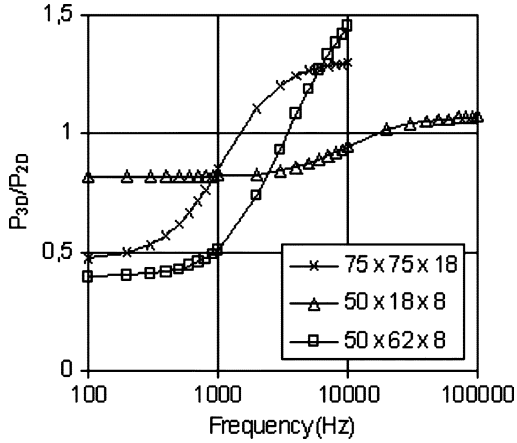

Fig. 5. Ratio between the 3-D and 2-D FEM calculated eddy-current losses for three magnet sizes as a function of frequency.

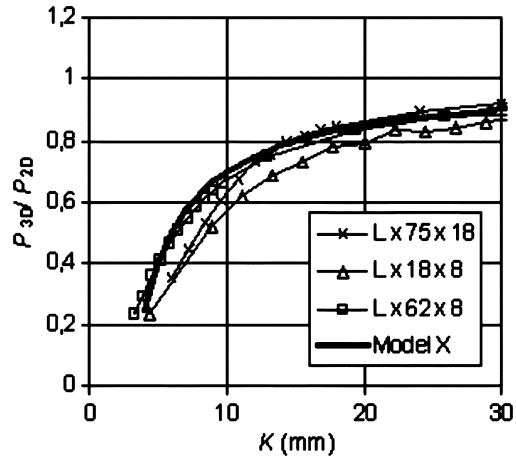

Fig. 6. Relative loss between 3-D and 2-D as a function of K in (1) for magnet A, B, and C. The input frequency used was 100 Hz. The thick black curve is fitted to the data. The fitting function is called model X in this paper.

between the 3-D and 2-D cases of three different magnets shows quite a similar behavior, if it is plotted as a function of

$$K = \frac{hL}{w} \tag{1}$$

where

h	magnet thickness (mm);
L	magnet length (mm);
w	magnet width (mm) (Fig. 6).

C. Curve Fitting

A curve fitting was made to the data in Fig. 6. It was noted that the following function gives quite a good agreement with the simulated results while it also is quite simple

$$\frac{P_{3\mathrm{D}}}{P_{2\mathrm{D}}} = 1 - \mathrm{C}_2 \frac{w}{hL} = 1 - \mathrm{C}_2 \frac{1}{K} \tag{2}$$

TABLE I
TRANSVERSAL RESISTIVITIES AND CURVE FITTING DATA OF $SmCo_5$, Sm_2Co_{17}, AND Nd-Fe-B MATERIALS [9]

Material	b in (3) $\cdot 10^{-3}$	a in (3)
$SmCo_5$	1.48 μΩm/°C	0.50 μΩm
Sm_2Co_{17}	0.94 μΩm/°C	0.75 μΩm
Nd-Fe-B	0.90 μΩm /°C	1.25 μΩm

where C_2 = constant: 3 mm.

This function will be called model X later in this text. Of course, the use of this function is restricted to low frequencies as can be seen from Fig. 5.

V. SUGGESTED 2-D/3-D CORRECTION

In this section, a model is suggested to improve the accuracy of 2-D FEM eddy-current analysis by introducing a correction factor to modify the resistivity of permanent-magnet material.

A. Anisotropy

The resistivity of sintered Nd-Fe-B, $SmCo_5$, and Sm_2Co_{17} is anisotropic [9]. The resistivity is different in the magnetic orientation direction of the magnetic material than perpendicular to the orientation direction (transversal resistivity). Normally, the eddy currents circulate in a permanent magnet in an electric machine in a plane perpendicular to the orientation direction and thus only the transversal resistivity should be considered in 2-D FEM eddy-current calculations. Only in very accurate eddy-current calculations in 3-D, the anisotropic resistivity must be considered [13].

B. Temperature Dependence

The transversal resistivity of modern high energy-product permanent-magnet materials as a function of temperature is a relatively linear function over the temperature range of interest for most electric machines. The coefficients a and b for linear equation (3) for resistivity for sintered rare-earth magnets can be found in Table I based on the measurements by Ruoho *et al.* [9]

$$\rho = \mathrm{b} \cdot T + \mathrm{a}. \tag{3}$$

C. 3-D/2-D Correction

In this paper, three analytical models and one curve-fitting model based on numerical calculations are developed to improve the 2-D calculation accuracy. The 3-D/2-D-correction factor F is calculated as follows:

$$\mathrm{F} = \frac{P_{3\mathrm{D}}}{P_{2\mathrm{D}}}. \tag{4}$$

For example, the calculation formula to make the 3-D/2-D-correction based on model A is

$$\mathrm{F} = \frac{P_{3\mathrm{D}}}{P_{2\mathrm{D}}} = \frac{3}{4} \cdot \frac{L^2}{w^2 + L^2}. \tag{5}$$

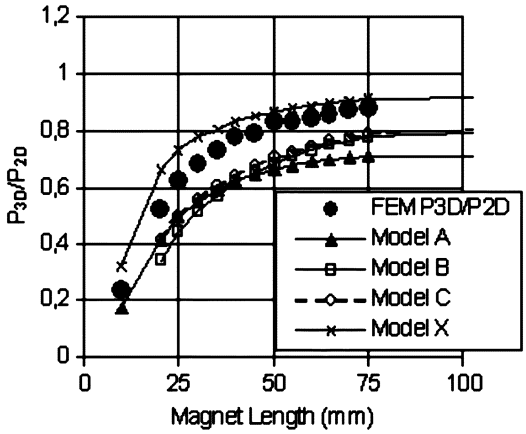

Fig. 7. Correction factor between 3-D and 2-D eddy-current losses for magnet B (width = 18 mm, thickness = 8 mm) as a function of magnet length calculated with FEM and with models A, B, C, and X. The input frequency in FEM model was 100 Hz.

This equation has been obtained by dividing (A3) by (A2) (see the Appendix). The correction factors according to models B and C can be derived in similar manners. The correction factor according to the numerical calculations, model X, is mentioned earlier in (2). The correction factors calculated with different models as functions of magnet length with fixed width and thickness are presented in Fig. 7. A FEM-calculated correction factor for a certain magnet size (length: varying, width: 18 mm, height: 8 mm) is also presented in Fig. 7 for comparison purposes.

D. Model

The model to adjust the resistivity of permanent magnets according to temperature and shape is simply

$$\rho = \frac{\mathrm{b} \cdot T + \mathrm{a}}{\mathrm{F}} \tag{6}$$

where a and b are coefficients (Table I) to calculate the transversal resistivity as a function of temperature and F is the 3-D/2-D-correction factor, which can be calculated by the analytical models or by the model X.

VI. MODEL COMPARISON

A six-pole machine (Fig. 8) [13] was simulated to verify the models A and X. Two different current input waveforms were used, while the machine was rotated at a constant speed of 6000 rpm. The sinusoidal 300 Hz input waveform causes a magnetic field that rotates at the same speed as the rotor, causing mostly an increase of space-harmonics. The sinusoidal 3 kHz input waveform is causing also time-harmonics, and thus it is more in the scope of this model verification. This problem is considered well resistance limited, because both the input frequencies are quite low. The results of the simulations are presented in Table II.

At first, the 2-D and 3-D eddy-current losses in permanent magnets were calculated using a resistivity of 1.32 $\mu\Omega$·m. The 2-D calculation gave higher losses than the 3-D calculation.

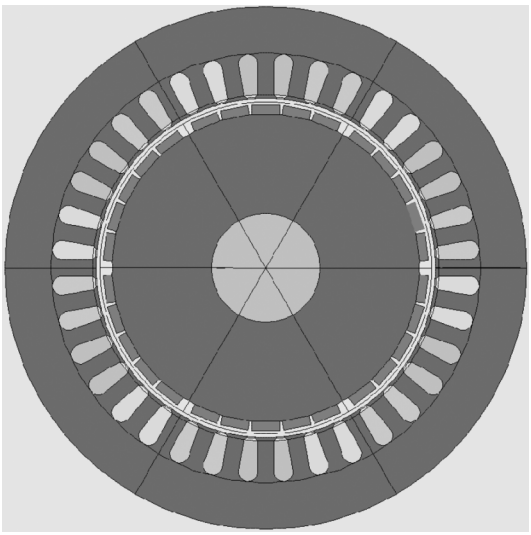

Fig. 8. Structure of the six-pole machine used to model eddy currents [13].

TABLE II
EDDY-CURRENT LOSS IN PERMANENT MAGNETS

Case	Input: 300 Hz, 92 A	Input: 3 kHz, 9.2 A
3D (ρ=1.32 μΩm)	45.49 W [13]	121.31 W [13]
2D (ρ=1.32 μΩm) (difference to 3D)	77.9 W [13] (+71 %)	168.4 W [13] (+39 %)
Corrected: model A 2D (ρ=2.13 μΩm) (difference to 3D)	51.1 W (+12 %)	110.5 W (-8.9 %)
Corrected: model X 2D (ρ=1.89 μΩm) (difference to 3D)	57.1 W (+26 %)	123.3 W (+1.6 %)

The difference was $+110\%$ for the 300 Hz input and $+39\%$ for the 3 kHz input. Then, the 2-D calculations were repeated with the modified resistivities. The magnet size of this machine was $30 \times 13.5 \times 4.5$ mm^3 (length × width × thickness) causing the following correction factors: 0.62 by model A and 0.70 by model X. The modified resistivities resulted 2.13 $\mu\Omega$·m and 1.89 $\mu\Omega$·m, respectively.

The 2-D calculations of eddy-current losses in the permanent magnets with the modified resistivity showed an improved accuracy when compared to 3-D calculations. With model A, the difference in eddy-current losses was $+12\%$ with the 300 Hz input and -8.9% with 3 kHz. With model X, the result differences were $+25\%$ and $+1.6\%$, respectively.

The models A, B, C, and X were developed to improve the calculation accuracy of eddy currents caused by time-harmonics in 2-D FEM calculations. This explains why the accuracy with the 300 Hz input remained lower after the correction: the 300 Hz input does not cause time-harmonics in this design. With 3 kHz-input, however, the calculation accuracy improved significantly: from $+39\%$ to $+1.6\%$, when model X was used.

In machine designs, where the time-harmonics are the major source of eddy currents in permanent magnets, the 2-D calculation accuracy of eddy-current losses in permanent magnets can be significantly increased by using a resistivity value, which is modified according to the shape of the permanent magnet.

VII. CONCLUSION

Three analytical models to estimate the eddy-current loss difference in 3-D and 2-D calculations by magnet shape were derived. A generic numerical model for FEM calculations was developed to study the same problem. A curve-fitting model based on the numerical calculations was established.

A model to improve the 2-D FEM eddy-current loss calculation accuracy was suggested based on adjusting the magnet resistivity according to the temperature and shape of magnets. The models were tested by calculating the eddy-current losses of a permanent-magnet motor with FEM. The calculations were performed in 3-D and in 2-D. The 2-D calculations were repeated with adjusted magnet resistivity. It was discovered that in machine designs where the major source of eddy currents in permanent magnets is caused by the time-harmonics, a significant improvement in the 2-D calculation accuracy of the eddy-current losses in permanent magnets can be achieved with the methods proposed.

APPENDIX I

Analytical equations for the total eddy-current losses in a permanent magnet in 2-D geometry and in 3-D geometry according to models A, B, and C are presented in this Appendix. The losses are calculated with the following assumptions.

- The magnetic flux density B is uniform throughout a magnet.
- The direction of B is perpendicular to the plane formed by dimensions L and w.
- The problem is resistance limited, i.e., the frequency is relatively low.
- The eddy current flows in one plane, i.e., the eddy-current density is the same through the magnet thickness h.

2-D Case

In the 2-D case there is an additional assumption, according to which all end-effects of eddy currents are neglected: The eddy-current loss density in a magnet in 2-D case is

$$\frac{P}{V} = \frac{1}{12} \cdot \frac{1}{\rho} \cdot w^2 \cdot \frac{\partial^2 B}{\partial t^2} \tag{A1}$$

where

P eddy current loss (W);

V $whL =$ magnet volume (m^3);

ρ electric resistivity ($\mu\Omega$·m);

w magnet width (m);

L magnet length (m);

h magnet thickness (m);

B magnetic flux density (Vs/m^2);

t time (s).

Equation (A1) is derived in [11] and [12].

Thus, the eddy-current loss power in a magnet is

$$P_{2-D} = \frac{1}{12} \cdot \frac{1}{\rho} \cdot w^3 h L \cdot \frac{\partial^2 B}{\partial t^2} \tag{A2}$$

3-D Case: Model A

In model A, the eddy current takes a rectangular path presented in Fig. 3. The eddy-current loss power in a magnet according to model A can be derived as follows: According to Faraday's law:

$$\oint \vec{E} \cdot d\vec{l} = -\frac{d}{dt}\Phi = -\frac{d}{dt} \iint_S \vec{B} \cdot \vec{n}\, dS.$$

If the resistivity is isotropic constant, and if the flux density is uniform over the integration surface, the following applies:

$$\oint \vec{J} \cdot d\vec{l} = -\frac{1}{\rho}\dot{B} \iint_S dS.$$

When this is applied to a geometry described in Fig. 9, the following relation is obtained:

$$2(J_x \cdot 2x + J_y \cdot 2y) = -\frac{1}{\rho}\dot{B} \cdot 4xy$$
$$J_x \cdot x + J_y \cdot y = -\frac{1}{\rho}\dot{B} \cdot xy.$$

Because of the geometry, the variables x and y and quantities J_x and J_y are related as follows:

$$y = \frac{w}{L}x, \quad J_y = \frac{w}{L}J_x.$$

The eddy-current loss power in a magnet is

$$P = \rho \cdot h \cdot 4 \left[\iint_{S1} J_x^2 dS + \iint_{S2} J_y^2 dS \right]$$
$$P = \rho \cdot h \cdot 4 \left[\int_{y=0}^{w/2} J_x^2 \cdot x(y) \cdot dy + \int_{x=0}^{L/2} J_y^2 \cdot y(x) \cdot dx \right].$$

When J_x and J_y are substituted, the equation takes the following form:

$$P = \rho \cdot h \cdot 4 \left[\int_{y=0}^{w/2} \left(-\frac{\dot{B}}{\rho} \cdot y \cdot \frac{L^2}{L^2 + w^2} \right)^2 \cdot \frac{L}{w} y \cdot dy + \int_{x=0}^{L/2} \left(-\frac{\dot{B}}{\rho} \cdot x \cdot \frac{w^2}{L^2 + w^2} \right)^2 \cdot \frac{w}{L} x \cdot dx \right].$$

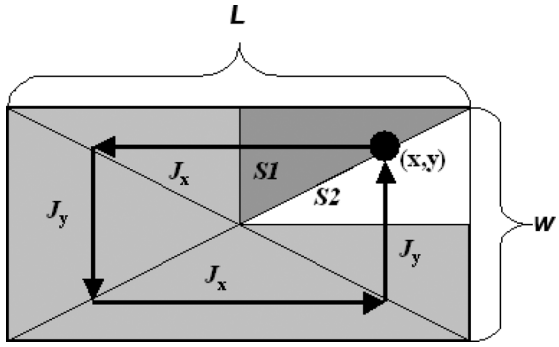

Fig. 9. Geometry used to derive the equations for model A.

After integration, the eddy-current loss power in a magnet according to model A is solved:

$$P = \frac{1}{16} \cdot \frac{1}{\rho} \cdot \frac{w^3 L^3 h}{w^2 + L^2} \cdot \frac{\partial^2 B}{\partial t^2}. \tag{A3}$$

3-D Case: Model B

In model B, the eddy current takes a straight path in the middle part of a magnet and a circular path at the magnet ends. The path is presented in Fig. 3. The equation for the eddy-current loss according to model B can be derived in similar manners than the equation for the model A. The eddy-current loss power in a magnet according to model B is

$$P = \frac{1}{\rho} \cdot h \cdot \begin{bmatrix} (L-w)^4 \cdot \left(\begin{array}{l} \frac{\pi}{128} + \frac{1}{16\pi} + \frac{1}{4\pi^2} - \frac{1}{16} \\ + \frac{1}{\pi^3} \\ \cdot \left(\begin{array}{l} -\frac{1}{2}\ln(2) - \frac{1}{2}\ln(L-w) \\ + \frac{1}{2}\ln(2L - 2w + \pi L - \pi(L-w)) \end{array} \right) \end{array} \right) \\ + (L-w)^3 \cdot \left(-\frac{\pi}{32} - \frac{1}{4\pi^2} + \frac{3}{16} - \frac{1}{8\pi}\right) \cdot L \\ + (L-w)^2 \cdot \left(\frac{3\pi}{64} + \frac{1}{16\pi} - \frac{3}{16}\right) \cdot L^2 \\ + (L-w) \cdot \left(\frac{1}{16} - \frac{\pi}{32}\right) \cdot L^3 \\ + \frac{\pi}{128} \cdot L^4 \end{bmatrix} \cdot \frac{\partial^2 B}{\partial t^2}. \tag{A4}$$

Equation (A4) was derived using a computer.

3-D Case: Model C

In model C, the eddy current takes a rectangular path presented in Fig. 3. The equation for the eddy-current loss according to model C can be derived in similar manners than the equations for the models A and B. The eddy-current loss power in a magnet according to model C is

$$P = \frac{1}{\rho} \cdot h \begin{bmatrix} (L-w)^4 \cdot \frac{1}{128} \cdot \ln\left(\frac{L+w}{L-w}\right) \\ + (L-w)^3 \cdot \frac{1}{64} \cdot L \\ + (L-w)^2 \cdot \frac{1}{64} \cdot L^2 + \\ - (L-w) \cdot \frac{1}{16} \cdot L^3 \\ + \frac{1}{32} \cdot L^4 \end{bmatrix} \cdot \frac{\partial^2 B}{\partial t^2}. \tag{A5}$$

Equation (A5) was derived using a computer.

ACKNOWLEDGMENT

This work was supported by Finnish Cultural Foundation, Research Foundation of Helsinki University of Technology, Ulla

Tuomisen Saüaütioü and High Technology Foundation of Satakunta. S. Ruoho would like to thank M.Sc. (Tech) Riku Mattila for assistance.

REFERENCES

[1] M. Rosu, J. Saitz, and A. Arkkio, "Hysteresis model for finite-element analysis of permanent-magnet demagnetization in a large synchronous motor under a fault condition," *IEEE Trans. Magn.*, vol. 41, no. 6, pp. 2118–2123, Jun. 2005.

[2] J. D. Ede, K. Atallah, G. W. Jewell, J. B. Wang, and D. Howe, "Effect of axial segmentation of permanent magnets on rotor loss in modular permanent-magnet brushless machines," *IEEE Trans. Ind. Appl.*, vol. 43, no. 5, pp. 1207–1213, Sep./Oct. 2007.

[3] J. L. Kirtley, M. Tolikas, J. H. Long, C. W. Ng, and R. Roche, "Rotor loss models for high speed PM motor-generators," in *Proc. ICEM*, 1998, pp. 1832–1837.

[4] M. Markovic and Y. Perriard, "Analytical solution for rotor eddy-current losses in a slotless permanent-magnet motor: The case of current sheet excitation," *IEEE Trans. Magn.*, vol. 44, no. 3, pp. 386–393, Mar. 2008.

[5] M. Markovic and Y. Perriard, "An analytical determination of eddy-current losses in a configuration with a rotating permanent magnet," *IEEE Trans. Magn.*, vol. 43, no. 8, pp. 3380–3386, Aug. 2007.

[6] N. Kesavamutrhy and P. K. Rajagopalan, "The polyphase induction machine with solid iron rotor," *Trans. AIEE*, vol. 78, pp. 1092–1098, 1959.

[7] C. Deak, L. Petrovic, A. Binder, M. Mirzaei, D. Irimie, and B. Funieru, "Calculation of eddy current losses in permanent magnets of synchronous machines," in *Int. Symp. Power Electronics, Electrical Drives, Automation and Motion*, Jun. 11–13, 2008, pp. 26–31.

[8] C. Deak, A. Binder, and K. Magyari, "Magnet loss analysis of permanent-magnet synchronous motors with concentrated windings," in *Proc. ICEM*, 2006, p. 6, CD-ROM.

[9] S. Ruoho, M. Haavisto, E. Takala, T. Santa-Nokki, and M. Paju, "Temperature dependence of resistivity of sintered rare-earth permanent magnet materials," *IEEE Trans. Magn.*, submitted for publication.

[10] R. Liu, C. C. Mi, and D. W. Gao, "Modeling of eddy-current loss of electrical machines and transformers operated by pulsewidth-modulated inverters," *IEEE Trans. Magn.*, vol. 44, no. 8, pp. 2021–2028, Aug. 2008.

[11] H. Polinder and M. J. Hoeijmakers, "Eddy-current losses in the segmented surface-mounted magnets of a PM machine," in *IEE Proc.-Electr. Power Appl.*, May 1999, vol. 146, no. 3, pp. 261–266.

[12] H. Polinder and M. J. Hoeijmakers, "Eddy-current losses in the permanent magnets of a PM machine," in *IEE Conf. EMD97*, no. 444, pp. 138–142.

[13] S. Ruoho, J. Kolehmainen, and J. Ikäheimo, "Anisotropy of resistivity of Nd-Fe-B magnets—Consequences in eddy-current calculations," in *Conf. Proc. REPM'08*, pp. 87–90.

Sami Ruoho was born in Pori, Finland, in 1973. He received the M.Sc. degree in applied physics from the University of Turku, Finland, in 1997. He is now pursuing the Ph.D. degree at the Laboratory of Electromechanics, Helsinki University of Technology (TKK), Finland. His subject is the modeling of demagnetization of permanent magnets in permanent-magnet machines.

Since 2002, he has been working for Neorem Magnets Oy, a company manufacturing sintered Nd-Fe-B magnets in Finland as a Research Engineer and as an Application Engineer. During his studies he still works part time for Neorem Magnets Oy (www.neorem.fi).

Timo Santa-Nokki was born in Ulvila, Finland, in 1978. He received the M.Sc. degree in physics from the University of Jyväskylä, Finland, in 2004.

Currently, he is working at Prizztech Oy, Magnet Technology Centre, Pori, Finland. He is interested in computational methods and electromagnetic modeling.

Jere Kolehmainen was born in Kuopio, Finland, in 1972. He received the M.Sc. and Ph.D. degrees in theoretical physics from University of Jyväskylä, Jyväskylä, Finland, in 1996 and 2000, respectively.

Currently, he is working at ABB Oy, Motors, Vaasa, Finland. He is interested in synchronous and induction AC machines and electromagnetic modeling.

Antero Arkkio was born in Vehkalahti, Finland, in 1955. He received the M.Sc. (Tech.) and D.Sc. (Tech.) degrees from Helsinki University of Technology, Finland, in 1980 and 1988, respectively.

He has been a Professor of electrical engineering (Electromechanics) at Helsinki University of Technology (TKK) since 2001. Before his appointment as a Professor, he was a Senior Research Scientist and Laboratory Manager at TKK. He has worked with various research projects dealing with modeling, design, and measurement of electrical machines.